Electronics meets Biology

Sensors
Interfaces
Hybrids
Neuronal Networks

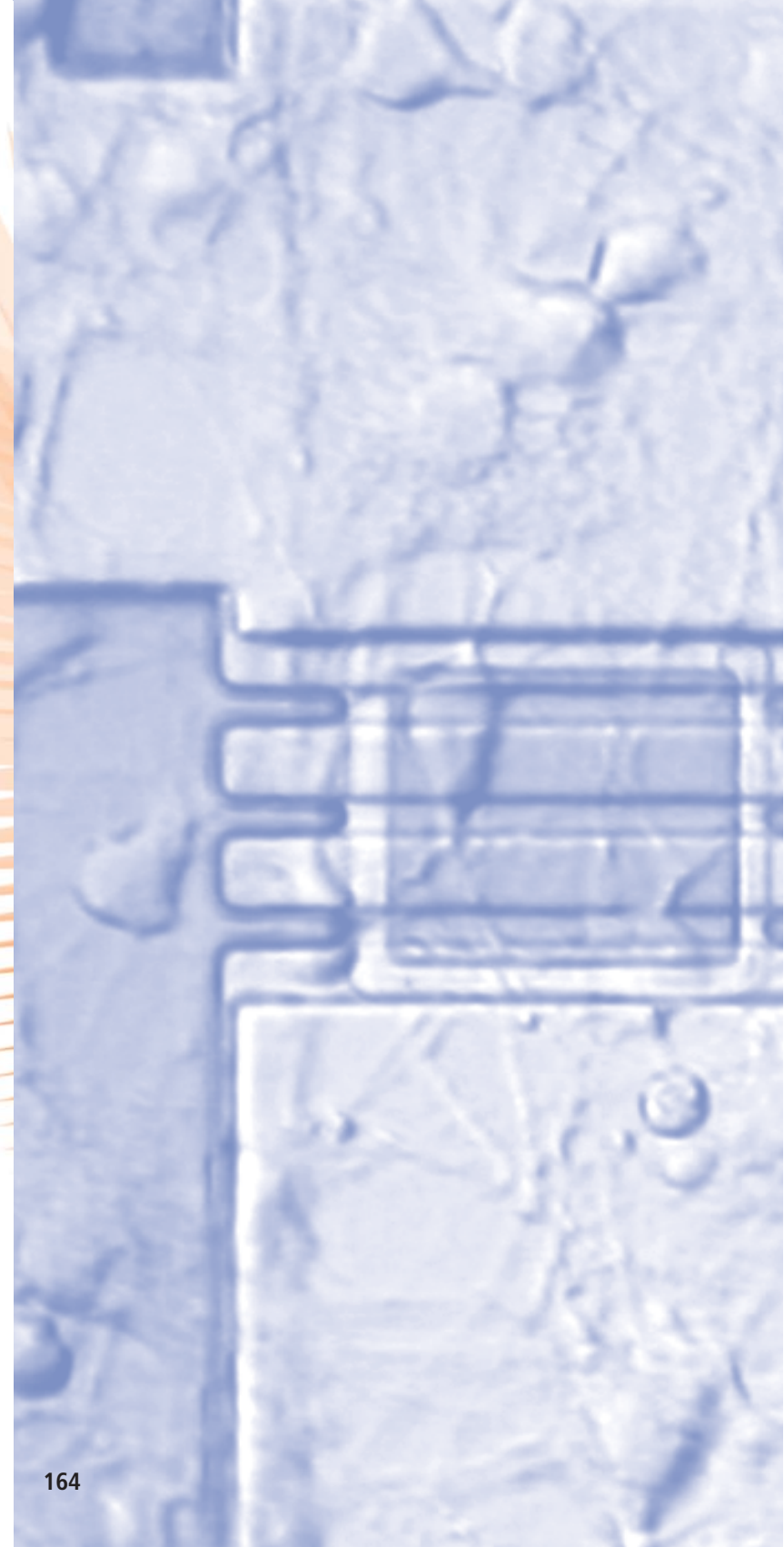

Silicon-based Biochemical Sensors

INTRODUCTION

Silicon-based microelectronics represents the platform of our modern information technology. In recent years, silicon technology has been utilized to couple data processing systems to chemical and biological structures, integrating ion-selective materials and simple biomolecules or even cells and cell systems.
The main advantage of these (bio-)chemical sensors is the high sensitivity and selectivity of their chemical and biological component as well as the possibility of miniaturization down to the nanometer scale. (Bio-)chemical sensors have been developed as rugged and reliable devices for the rapid and quantitative detection of specific analytes. For example, enzymes allow to monitor the blood glucose concentration of diabetic patients, a pH electrode may adjust the proper fermentation routine for cheese production and sensors and catalysts control the car pollution. (Bio-)chemical sensors constitute an interdisciplinary interface between the environment and data processing systems. Moreover, because these sensors can be designed in a modular concept, the combination of single sensors to sensor arrays is possible.

APPROACH

We present some examples of new silicon-based (bio-) chemical sensors, which have been developed in a collaboration between ISG (FZJ) and the University of Applied Sciences Aachen (Jülich division):

- capacitive field-effect sensors as a combination of ionophores or enzymes and silicon technology,
- a silicon-based multi-parameter hybrid ion-sensitive FET (ISFET) module suitable for sensor arrays,
- a beetle/chip biologically sensitive field-effect transistor (BioFET) as a first step towards a bioelectronic device with extraordinary sensory abilities.

All described (bio-)chemical sensors utilize the field effect to transfer the detected (bio-)chemical information to an electrical signal.

RESULTS

Capacitive field-effect sensors combine the physical field effect as transducer principle and the chemical recognition mechanism of ion-selective electrodes. In this sensor the charge carrier distribution at the interface between insulator and semiconductor (for example SiO_2 and p-type Si) can be either controlled by an external dc and ac voltage (Fig. 1a) or a dc voltage combined with a probe light (Fig. 1b). Depending on the read-out principle of the capacitance of the space charge layer, the sensor is called EIS (electrolyte-insulator-semiconductor) sensor or LAPS (light-addressable potentiometric sensor). The formation of charged adsorbed species at the phase boundary sensitive layer/electrolyte results in an electrochemical interaction, which is in both cases accompanied by a measurable surface potential. Usually, the sensor is operated vs. a miniaturized Ag/AgCl reference electrode. Within the last years, different sensitive layers and substrate combinations have been developed in our group: pH-sensitive layers consisting of Al_2O_3 or Ta_2O_5 allow to determine pH variations with high accuracy in aqueous solutions in the concentration range from pH 2 to pH 12. Here, the pulsed laser deposition technique has been introduced as an innovative film preparation method. The average pH sensitivity of the microfabricated pH sensors is about 56-58 mV/pH and the long-term stability extends to more than 3 years.

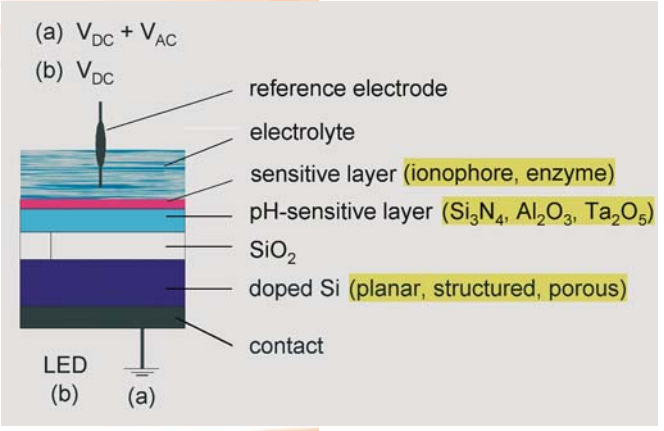

Fig. 1
Sketch of a capacitive field-effect sensor for the determination of ions or biomolecules in aqueous test samples. Various sensitive layers and materials as well as substrate configurations have been developed. The field-effect sensor can work as an EIS (electrolyte-insulator-semiconductor) structure (a) or as LAPS (light-addressable potentiometric sensor) device (b).

The immobilization of additional enzyme layers (e.g., penicillinase, organophosphorus hydrolase, alliinase) on top of the microfabricated pH sensor leads to a simple and successful biosensor concept. The enzymes take advantage of the catalytic hydrolyzis of their biological substrate releasing H^+ ions, which can be detected with high efficiency by the underlying pH-sensitive layer. Thus, the resulting sensor signal is a measure of the substrate concentration in the solution: the enzyme penicillinase catalytically converts penicillin, while organophosphorus hydrolase is sensitive towards pesticides, and alliinase detects garlic.

By using these three enzymes, the applications span the areas biotechnology, environmental monitoring and biomedicine. Instead of biomolecules, specific ionophores supported in a PVC-based membrane as sensitive layer allow to determine various mono- and divalent ions, like K^+, Li^+, Cs^+, Mg^{2+} and Ca^{2+}.
The major task, however, in view of the combination of biomolecules and microelectronics is the stable coupling of the enzymes onto the field-effect structures. Complex surface chemistry (immobilization by heterobifunctional cross-linking) or sophisticated physical binding, like the structuring of the sensor surface by etching, is developed. For example, we favour porous silicon with its sponge-like structure, because the pore size and geometry can easily be tailored for the attachment and anchoring of biomolecules, permitting the design of a three-dimensional (bio-)chemical sensor.

For the capacitive field-effect sensors, the signal is derived from capacitance-voltage measurements, as shown for the EIS sensor in Fig. 2a. When a substrate variation occurs in the test solution, e.g. from c_1 to c_2, the curves shift along the abscissa, according to the sensitivity of the transducer. The value of the shift gives the variation in the concentration. For the LAPS device, one can obtain the same concentration-dependent shift, but with the distinction that the photocurrent serves as the sensor signal (Fig. 2b).
The requirement to measure several parameters in complex mixtures consequently leads to the development of miniaturized sensor arrays or systems, like the µTAS (micro total analysis system) or "lab-on-a-chip" sensors. A sensor system for the multiparameter detection can be built-up monolithically or hybrid. Different concepts for hybrid modules are discussed in literature. However, all modules contain both (bio-)chemical sensors and physical sensors for the additional control of physical parameters as temperature, conductivity, flow rate or liquid level. Since the design of the physical sensors differs from that of the (bio-)chemical sensors, the complete sensor system needs a more complicated fabrication technology and read-out scheme.

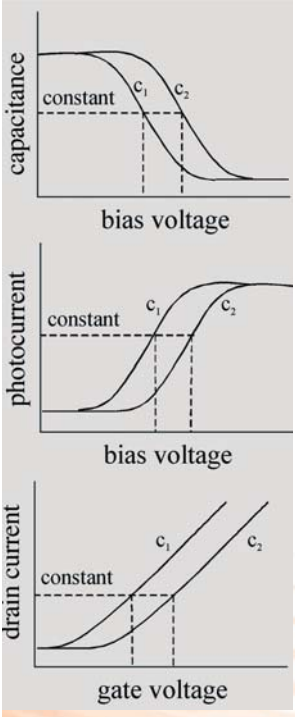

EIS (a)

LAPS (b)

ISFET (c)

Fig. 2
Schematic sensor response of an EIS sensor (a), a LAPS device (b) or an ISFET (c) with varying ion concentrations in the solution. The concentration to be determined increases from c1 to c2.

Fig. 3
The multi-parameter hybrid module enables the detection of both (bio-)chemical and physical quantities (a). Video microscopic picture of the developed hybrid sensor module consisting of two ISFET chips and an ion generator onto a printed circuit board before encapsulation by an epoxy resin (b).

In order to ease these demands, we have suggested a novel approach for a multi-functional hybrid sensor module using the same transducer principle and structure for both (bio-)chemical and physical parameters. In this hybrid module, the (bio-)chemical sensor can serve as physical sensor and thus, the number of obtained (bio-)chemical and physical parameters exceeds the number of sensors. The setup is called a "high order system". Fig. 3a shows the schematic configuration of such a hybrid module with a Ta_2O_5-gate ISFET as transducer. The module (Fig. 3b) consists of two ISFETs, or one ISFET and one EnFET (enzyme-

(a)

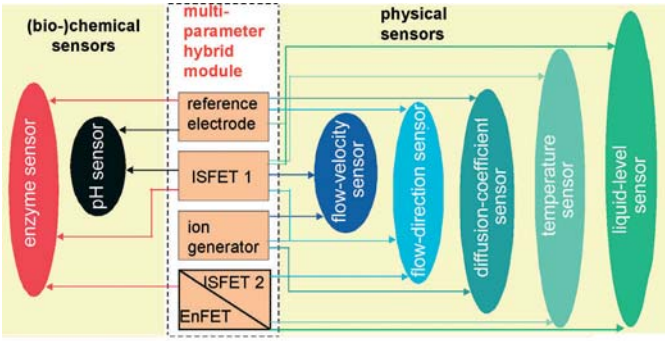

(b)

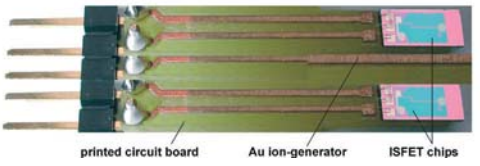

modified FET), and an ion generator (Au or Pt). On the basis of this module, it is possible to realize at least three (bio-)chemical sensors (pH, ion and/or enzyme sensor), five physical sensors (flow velocity, flow direction, diffusion coefficient, temperature, liquid level) and one actuator (ion or gas generator). The multi-functionality of this array is achieved by different sensor arrangements and operation modes. Moreover, this array minimizes the influence of various disturbing factors by using a differential measuring set-up. For this ISFET-type array, the concentration-dependent sensor signal can be evaluated by the shift of the gate voltage at a fixed drain current (Fig. 2c).
The beetle-chip BioFET is a completely new type of biosensor in which the antenna of an insect is coupled via an electrolyte to

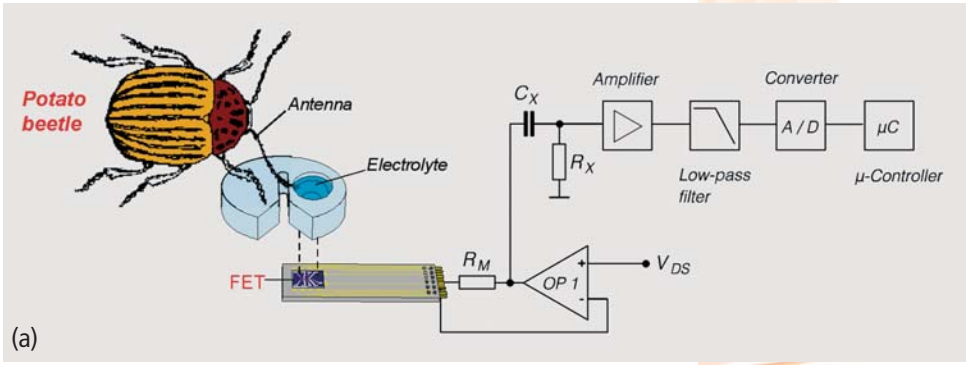

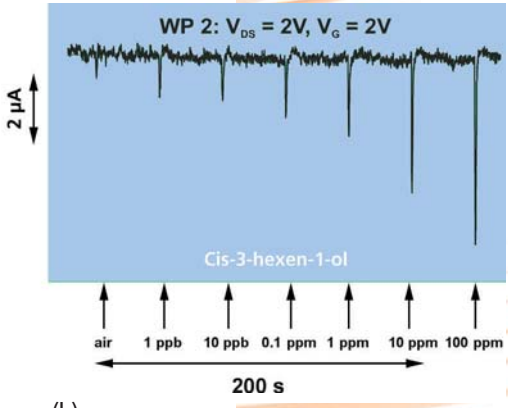

Fig. 4
Beetle-chip sensor as an example of a bioelectronic field-effect sensor. The tip of the beetle's antenna contacts the gate of the FET via an electrolyte; the resulting drain current changes are amplified (a). Characteristic drain current changes (abscissa) derived from different odour concentrations (e.g., Cis-3-hexen-1-ol) as a function of time (b).

the gate of a FET (Fig. 4a). Such a bioelectronic interface possesses extraordinary sensory abilities, because the biological part has been optimized by millions of years of evolution. The organic compound detected by the beetle's antenna initiates a recognition process that results in a net potential: if odour molecules reach the antenna by diffusion, they are able to bind to specific odour-binding proteins in the neurones of the antenna. The complex of odour and protein then opens ion channels in the cell membranes, yielding membrane potentials. Triggered by these protein-driven reactions, an electrical polarization develops, resulting in a sum dipole over the whole antenna. As a consequence, the channel conductivity of the FET and thus its drain current is modulated (Fig. 4b). The more intense the odour stimulus is, the stronger are the recorded signals.
By using the antennae from selected insects (e.g., Colorado potato beetle, steelblue jewel beetle), different odours such as Cis-3-hexen-1-ol, guaiacol and 1-octen can be detected.
Plant damages by the attack of a potato beetle can be discriminated by setting a threshold, which allows to distinguish

between healthy and damaged plants. Besides the detection of plant diseases, an optimized use of pesticides and a more efficient food protection due to the determination of mycotoxine-producing organisms,e.g., becomes feasible. A BioFET based on the antenna of the steelblue jewel beetle can specifically detect burning wood as in forest fires with unrivalled sensitivity and a superior selectivity, as compared to semiconductor gas sensors. A "library" with different beetle species and their odour detection spectra will broaden the field of application. It is a remaining challenge to isolate of the receptor molecules inside the antennae in order to fabricate these biosensors without the use of the beetles or their antenna. Then the entire molecular recognition centre will be reconstructed on the silicon microchip, leading to the development of "nano-biosensors".

ACKNOWLEDGEMENTS

The author thanks Y. Ermelenko, M. Keusgen, A. Mulchandani, A. Poghossian, P. Schroth, J. Schubert, S. Schütz, A. Steffen, M. Thust and T. Yoshinobu for technical support and valuable discussions.

REFERENCES

(1) "Novel approaches to design silicon-based field-effect sensors"
M.J. Schöning in: J.W. Schultze, T. Osaka, M. Datta (eds.) Electrochemical Microsystem Technologies, New Trends in Electrochemistry Vol. 2, Taylor & Francis, 2002, London New York, pp. 384-408.

(2) "(Bio-)chemical and physical microsensor array using an identical transducer principle"
A. Poghossian, H. Lüth, J.W. Schultze, and M.J. Schöning Electrochim. Acta 47 (2001) 243-249.

(3) "Electrochemical methods for the determination of chemical variables in aqueous media"
M.J. Schöning, O. Glück, and M. Thust
in: J.G. Webster (ed.) The measurement, Instrumentation and Sensors Handbook, CRC Press, 1999, Boca Raton and Springer-Verlag Heidelberg, pp. 70/1-70/49.

AUTHOR

Michael J. Schöning
(ISG, FZJ, and University of Applied Sciences Aachen, Jülich Division)

Cell-Transistor-Hybrid Systems

INTRODUCTION

Biological cells are able to receive, process, and transmit information. Connecting these cells to micro-electronic circuits opens up exciting new perspectives in bioelectronics, information technology, medical engineering and in sensor development. Living cells possess receptors of unmatched sensitivity that detect external signals of chemical nature (nutrients, hormones, neurotransmitters, changes in proton- or ion-concentration, etc.) or physical stimuli as a change in temperature, light, mechanical force, or even electromagnetic fields. These input parameters are processed by the cells. The internal "machinery" of the cell includes signal amplification cascades and logic connections of high non-linearity, but the details remain to be unveiled. The resulting output signal may generate many physiological reactions inside the cell, as the synthesis of specific molecules, a change in gene expression or the storage of certain substances. The output signals also allow the cell to communicate with its environment and with other cells.

APPROACH

In order to provide selective long-term cell-transducer interfaces in vitro, microtechnology is used for the development of planar arrays with large numbers of field-effect transistors or metal electrodes in the size of the individual cells. These arrays usually consist of a culture chamber with embedded chip. For metal-electrode arrays (MEAs), insulated conductor paths are patterned lithographically. Their opened metallic ends form the sensing electrodes. In addition, field-effect transistor (FET) arrays have been developed to record the electrical signals from cells. Modifications of standard FET fabrication processes lead to devices with metal-free gate electrodes. A variation of these devices is the so-called ion-sensitive field-effect transistor (ISFET). Its gate dielectric is modified to yield higher sensitivity for certain ions. Sufficient electrical coupling between the cell and the electrode for extracellular signal recording is achieved only if a cell or a part of a cell is located directly on top of the electrode.

Fig. 1(a)
Assembled and encapsulated FET. The chip with the 4x4 transistor array is mounted in the middle of a mini cell culture dish.

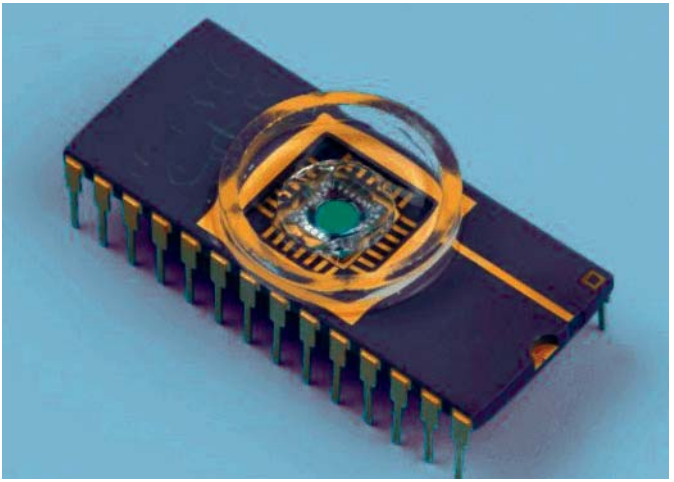

Fig. 1(b)
Micrograph of the array of 4x4 field-effect transistors used in these studies

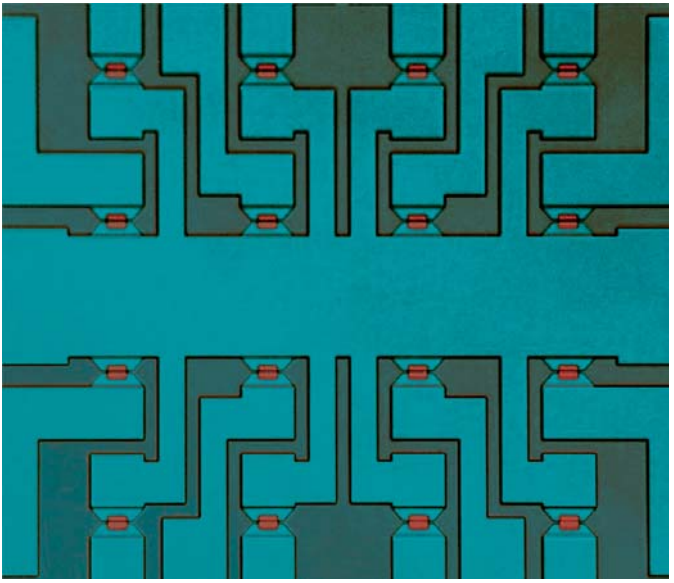

Figure 1(a) shows a photograph of the complete device with the active chip mounted onto a standard chip carrier. A mini-petri dish is sealed to the chip to allow the cells to be cultured in contact with the FET gate electrodes. A magnified picture of the chip surface is given in Fig. 1(b). Our device integrates 16 transistors in a 4x4 array. They share a common source but have individual drain connections for parallel read-out. The gate areas are covered by non-metallized SiO_2 , optimized for high sensitivity, low noise and low signal drift.

RESULTS

Prior to cell seeding, the chip surface has to be functionalized by a protein coating that promotes cell adhesion and survival and, if necessary, allows for cell patterning. The employed strategies to achieve this goal range from mere physisorption from solution to complex supramolecular interfacial multi-layer architectures.

The properly prepared chip surface can be used as a substrate for in-vitro cell culture. In particular we work with cardiac myocytes (heart muscle cells) and primary neurons, both from embryonic rats. The heart muscle cells offer the particular advantage that after random seeding they grow on the chip surface to a confluent monolayer. They establish both mechanical and electrical contacts between neighboring cells. Moreover, after a few days in culture they start to spontaneously contract and to fire action potentials, which are at first completely random. However, eventually one cells becomes the "pacemaker" and triggers all others of that population to generate a synchronized mechanical and electrical excitation pattern with a rather regular repetition rate of approx. 1 Hz. The excitation wave propagates across the cell layer with a velocity of approx. 0.15 m/sec. The action potential of an individual cel, can be monitored by a classical micropipette recording unit and shows the well known voltage-time profile given in Fig. 2(a), resulting from time-dependent contributions of Na^+-, K^+-, and Ca^{++}-currents across the cell membrane. The patch pipette recording shows an excellent signal-to-noise ratio. However, the cell does not survive that treatment longer than a few hours, and a multielectrode

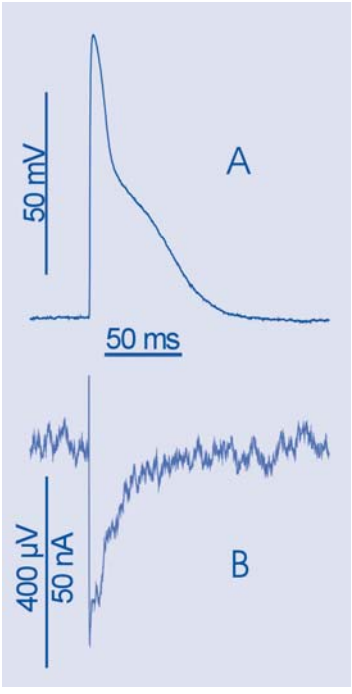

Fig. 2
Action potential recordings from a rat cardiac myocyte taken simultaneously with a glass microelectrode (A) and a FET (B).

Fig. 3
Micrograph of a random network of brain stem neurons cultured on the surface of a FET chip. One neuronal cell resides almost completely on the gate electrode of the transistor (triple gate structure).

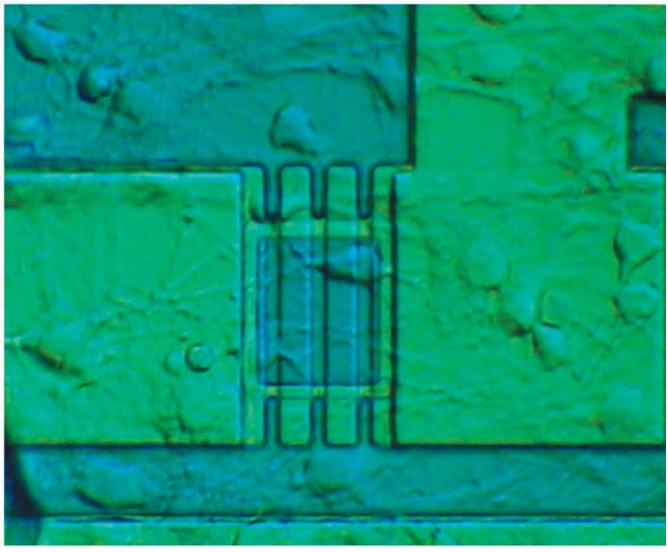

recording exceeding 3 electrodes/cell-culture at the same time is barely possible. Recordings by our FET devices (one example is given in Fig. 2(b), which is the simultaneously measured event of Fig. 2(a)) show lower amplitude and a higher noise level due to a weaker coupling of the cell to the gate electrode as compared to the patch pipette. However, they can be monitored for weeks, and with our present array design on 16 channels simultaneously. As an example for the possible application of this cell-transistor hybrid system, we recently demonstrated the influence of certain drugs known to stimulate the frequency of the heart beat. Isoproterenol (ISO), e.g., was shown to enhance the beat frequency of our myocyte monolayer. A full dose-response curve could be recorded within minutes. The limit for the response detection was shown to be at an ISO concentration of only 10^{-11} mol/liter !

After 4 days in culture, rat brain stem neurons randomly adhered to the substrate, with one neuron fortuitously positioned on top of a gate electrode (Fig. 3). It developed "healthy" dendrites and axons, the "receivers" and "transmitters" for cell-cell communication. These cells were sufficiently coupled to the gate electrode to allow for FET recording of an action potential that was triggered by a patch electrode, but formed a totally random network structure.

REFERENCES

"Electrical recordings from rat cardiac muscle cells using field-effect transistors"
C. Sprössler, M. Denyer, S. Britland, W. Knoll, A. Offenhäusser
Phys. Rev. E 60 (1999) 2171-2176

"Cell-transistor hybrid systems and their potential applications"
A. Offenhäusser and W. Knoll
Trends in Biotechnology 19 (2001) 62-66

"Cardiomyocyte-Transistor-Hybrids for Sensor Application"
S. Ingebrandt, C.-K. Yeung, M. Krause, A. Offenhäusser
Biosensors and Bioelectronics 16 (2001) 565

AUTHORS

Sven Ingebrandt, Andreas Offenhäusser

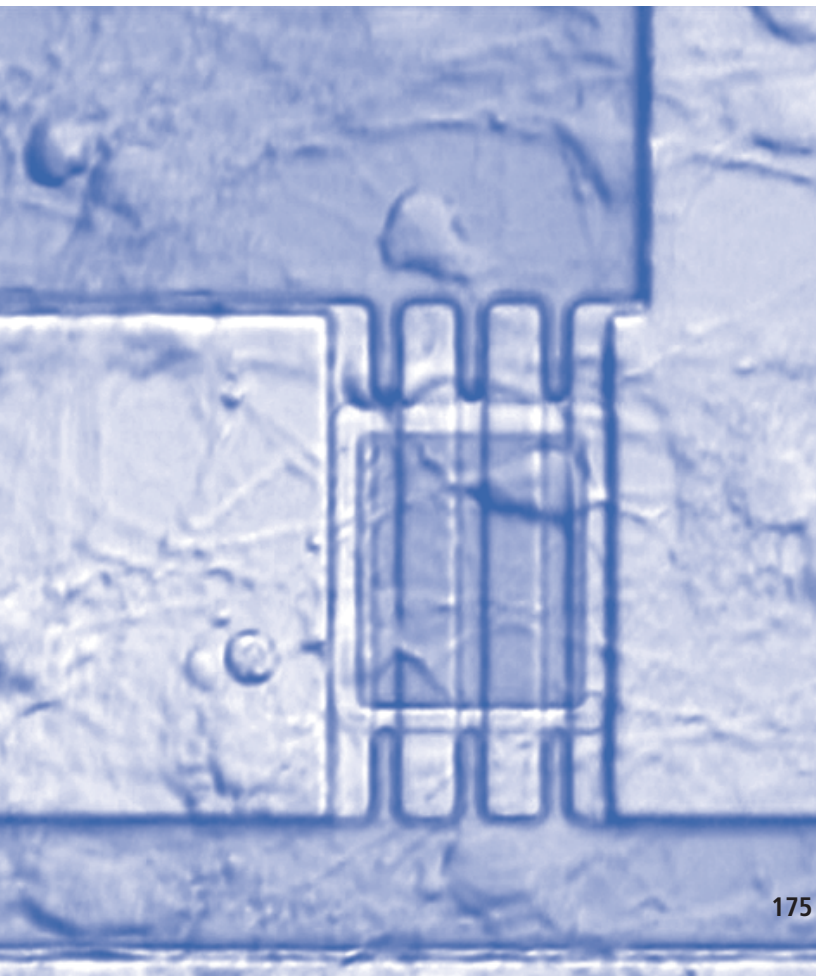

Biological Neuronal Networks

INTRODUCTION

The growth of neurons into networks of controlled geometry has numerous potential applications in cell-based biosensors, neuroelectronic circuits, neurological implants and pharmaceutical testing. It also permits fundamental biological studies about neuronal interactions. Within the neurons, differences in electrical potential encode information, and messages can be passed on to other neurons through chemical or electrical connections. In order to decipher the neural code, our aim is the construction of networks of neurons in culture, with each neuron connected to others through synapses. We intend to reproduce the connectivity of intact nervous systems. On the other hand, their interruption leads to a loss of physiological function. It is assumed that the messages passing across a synapse carry instructions for processing and possibly routing of the neuronal information. Therefore, we would like to test the effects of different connectivities and input messages on the neuronal output. These data possibly allow to establish a basic system to model the in vivo situation of neuronal processing as closely as possible.

APPROACH

Different techniques can be used to produce surface patterns for cell guidance of high spatial resolution down to the micrometer scale. Examples are standard photolithographical patterning, a combination of laser ablation techniques with lithographic masks or with topographic features. We have chosen the microcontact printing (μCP), because it is a comparatively simple and universal method for patterning biomolecules. A stamp is produced casting a silicone elastomer (polydimethylsiloxane, PDMS) in the desired pattern and then coated with a biomolecule solution to be transferred. After contacting the "inked" stamp with the substrate surface, the biomolecules are transfered to the predetermined pattern.

Microstamps for the experiments were produced by photolithography and molding. Applying UV-photolithography, master

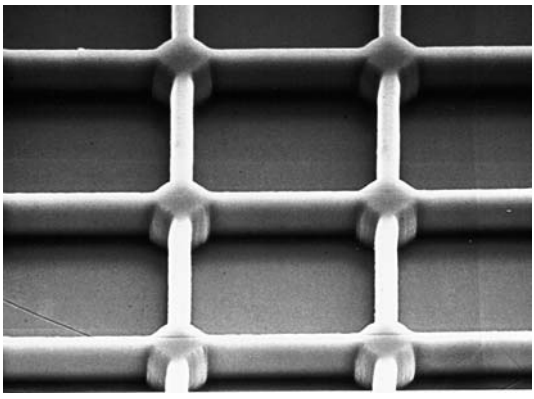

Fig. 1
Image of a PDMS stamp used for the neuronal cell patterning.

stamps were produced out of spin coated thick photoresist layers on silicon wafers. Polydimethylsiloxane (PDMS) microstamps were then fabricated curing the polymer on the master stamps (Fig. 1).

Inking took place by applying certain biomolecules as laminin dissolved in phosphate buffer. The inked stamp was dried in a soft nitrogen air stream and immediately pressed onto the substrate.

Line and grid patterns were applied. These patterns have nodes for the adhesion of cell bodies in equidistant steps of 100 µm in x-direction and 50 µm in y-direction. The nodes of the grid patterns are located at the intersections of the grid. The nodes of the line patterns are distributed along the lines. In order to study the influence of the pattern geometry on the cellular growth, patterns with varying line size and node size were chosen (Fig. 2).

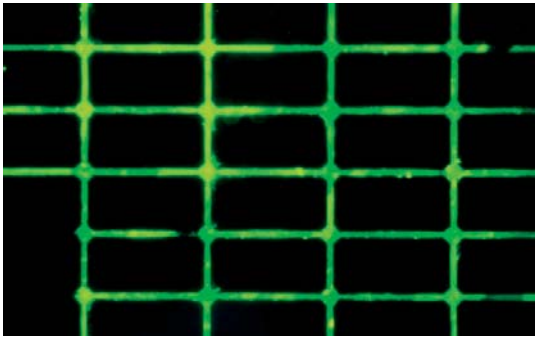

Fig. 2
Fluorescence image of an imprint of fluorescein-labeled biomolecules. The pattern consists of 5 µm wide lines crossing in 50 respective 100 µm. The crossing points consist of nodes of 12 µm in diameter.

RESULTS

Dissociated neurons from rat embryos were seeded onto micropatterned substrates. The substrates consisted of polystyrene as a highly hydrophobic background onto which a pattern made of physiological proteins had been applied as described before. The contrasting surface areas forced the cells to align themselves along the pattern and to extend their processes accordingly. We used grid patterns consisting of 4-6 µm wide lines and nodes that were 12-14 µm in diameter. In order to avoid the deposition of serum proteins onto the hydrophobic background, which would reduce the contrast between the two areas, a serum-free medium was used. As shown in Fig. 3, the aligning of the cell bodies onto the nodes was achieved to a very high degree, as well as the guidance of the growth process along the lines. In the resulting network, any given cell could physically contact and thus form synapses with its direct neighbours on the pattern. Apart from morphological

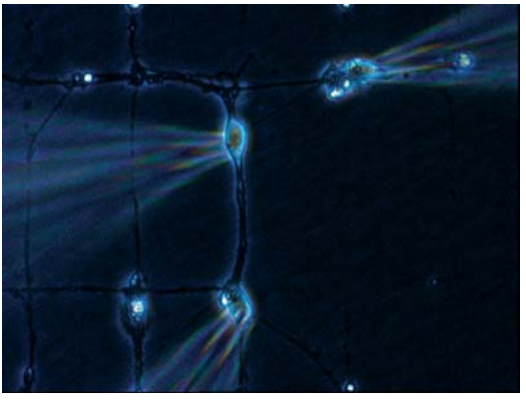

Fig. 3
Cortical neurons on grid patterns after 13 days in culture. Next to the cells, the patch-clamp electrodes used for the electrophysiological recordings are visible.

and electrophysiological evidence, the neuronal identity of the cells was confirmed by antibody staining, using an antibody against the neuron-specific cytoskeleton protein neurofilament-M. Our networks were stable for up to three weeks. After this time, the cells tended to overgrow the pattern and form connections across the non-permissive "forbidden" areas.

Electrophysiological recordings in the form of triple patch clamp measurements were performed to test the synaptic connectivity. Two to three neighbouring cells were patched simultaneously in the current clamp mode. An action potential was evoked in one

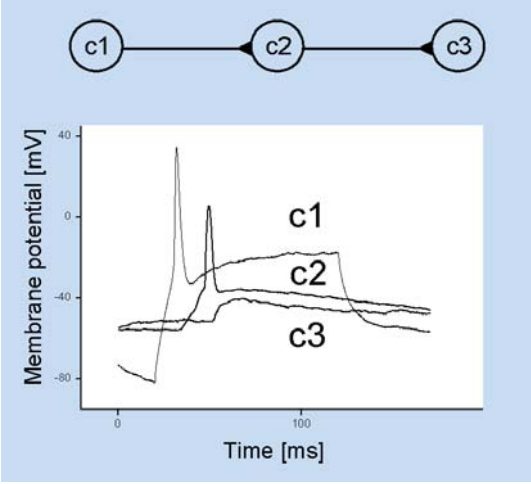

Fig. 4
Functional coupling recorded from cortical neurons. A presynaptic action potential (c1) induced a postsynaptic action potential (c2), which induced a postsynaptic depolarization (c3).
The start of the postsynaptic depolarisation was delayed by a specific time to the presynaptic spiking. This delay, which is specific for chemical synapses, is mainly caused by the time required for transmitter release, transmitter diffusion and postsynaptic ion channel gating.

cell by a depolarising current pulse and the resulting effect was monitored in the other cells. As shown before, small circuits of three cells communicating through two successive synapses could be found. A signal evoked in the first cell (c1) was transduced through the first synapse to the second cell (c2), resulting in an excitatory postsynaptic potential (EPSP), while no effect on the third cell (c3) was observed. An action potential evoked in c2 induced an EPSP in c3 through the second synapse, but not in c1, whereas an action potential in c3 had no effect on the other cells. This indicates a unidirectional connection from c1 via c2 to c3 through two synapses in succession. In another recording (Figure 4), stimulation of c1 resulted in an EPSP in c2 that was large enough to trigger an action potential, which in turn caused an EPSP in c3. In this recording, the signal travelled via two synapses through all three cells of the constellation.

In summary, our experiments demonstrate an excellent control of cell growth on patterned substrates, permitting a detailed tracing of of the electrical signal propagation. This will enable us to study the cellular communication code in increasingly complex networks.

REFERENCES

"Ordered networks of rat hippocampal neurons attached to silicon oxide surfaces"
M. Scholl, C. Sprössler, M. Denyer, M. Krause, K. Nakajima, A. Maelicke, W. Knoll, A. Offenhäusser
J. Neurosci. Meth. 104 (2000) 65

"Spot Compliant Neuronal Networks by Structure Optimized Micro-Contact Printing"
L. Lauer, Ch. Klein, A. Offenhäusser
Biomaterials 22 (2001) 1925

"Electrophysiological recordings of patterned rat brain stem slice neurons"
L. Lauer, A. Vogt, C. K. Yeung, W. Knoll, A. Offenhäusser
Biomaterials 23 (2002) 3123

AUTHORS

Simone Böcker-Meffert, Andreas Offenhäusser, Angela Vogt

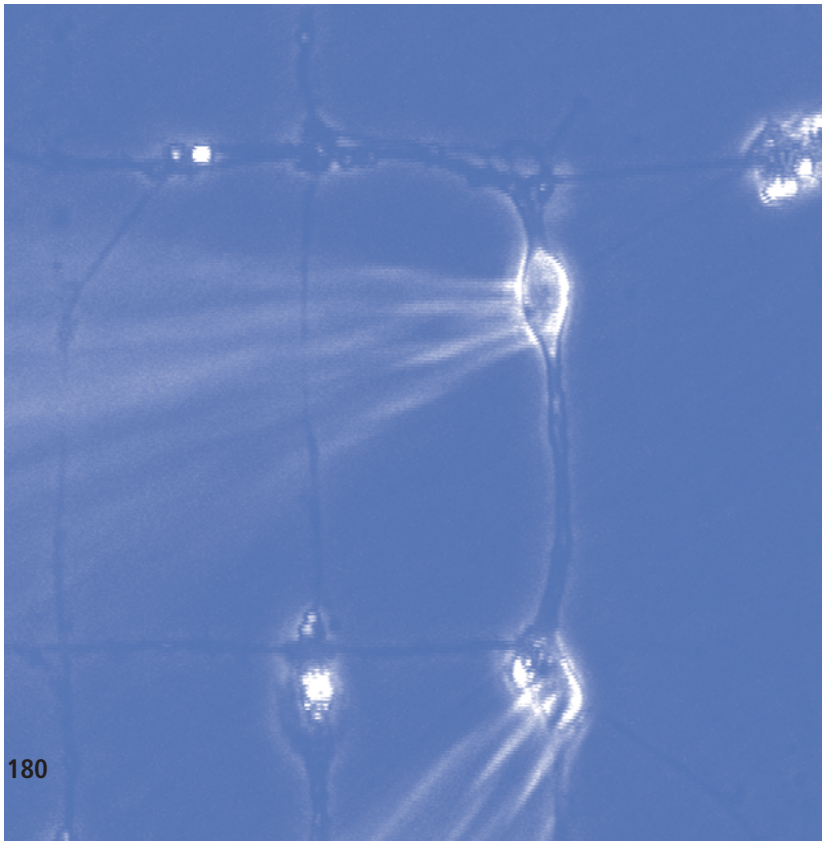

SQUIDs: The Ultimate Magnetic Sensors for Materials Characterization and Biomedical Diagnostics

INTRODUCTION

SQUIDs (**S**uperconducting **QU**antum **I**nterference **D**evices) are the most sensitive magnetic field or flux detectors known. For simplicity, they can be described as analog-to-digital converters of magnetic signals, quantized in units of the magnetic flux quantum, $\Phi_0 = 2.07 \times 10^{-15}$ Wb. An external feedback circuit is used to cancel the applied flux. Thus the SQUID operates as a null detector. Such an analog device can resolve very small fractions of the flux quantum, down to 10^{-6} Φ_0, permitting a magnetic field resolution of the order of a few fT/√Hz. SQUIDs are especially useful for low frequency magnetic signals. They are unmatched with respect to flux sensitivity. They permit the detection of the weak magnetic fields generated by biological currents, including heart or brain activities. Such a high sensitivity is achieved by the macroscopic coherence of the electronic wavefunction of the superconducting state. Therefore the SQUID sensor has to be cooled below the critical temperature of the superconducting material.

The discovery of the High Temperature Superconductors, especially YBaCuO, led to the development of SQUIDs which can be operated at a temperature of 77 K (liquid nitrogen) instead of 4.2 K (liquid helium). They allow a significant simplification of cryogenics with the ensuing reduction in investment and operating cost, and the simplification of handling and maintenance, including an increased portability. Small, reliable cryocoolers with a low level of vibration-induced und electromagnetic noise (e.g. Joule-Thomson or Pulse Tube) have been shown to be applicable. They constitute a practical cooling option for industrial SQUID applications.

APPROACH

Our sensors are based on radio-frequency (rf) SQUIDs. These devices consist of one Josephson junction in a superconducting

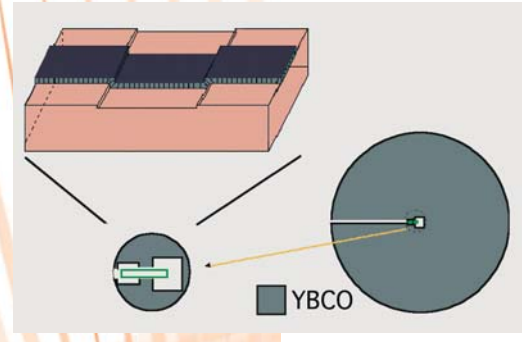

Fig. 1
Schematic of the SQUID layout.

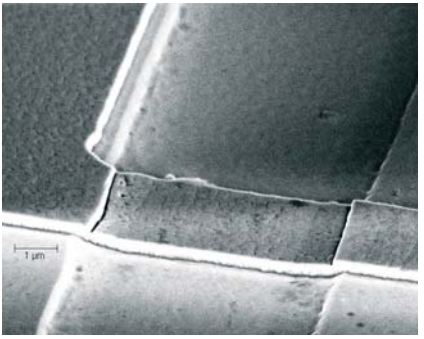

Fig. 2
SEM of the step edge junction of a SQUID.

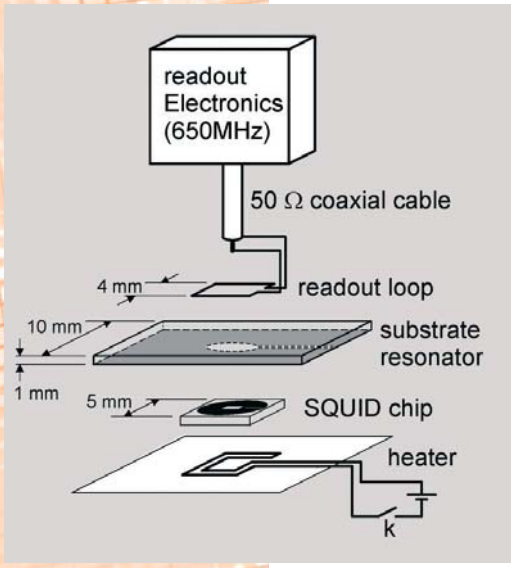

Fig. 3
Principle of substrate resonator SQUID.

ring. A well defined grain boundary constitutes a weak link within an epitaxial YBaCuO layer. These grain boundary junctions are prepared first by ion beam etching of a steep ditch into single crystal $LaAlO_3$ or $SrTiO_3$ substrates (1), see Fig. 1. Then epitaxial YBCO thin films are grown by laser ablation, forming the crucial step-edge grain boundary Josephson junction at the edge of the ditch (Fig. 2). The radio-frequency (rf) SQUIDs, consisting of single junction loops with a flux-focusing washer (Fig. 1), are photolithographically patterned using chemical etching. A 10 x 10 x 1 mm^3 $SrTiO_3$ substrate, acting as substrate resonator (2), serves as the tank circuit for SQUID readout and is positioned in flip-chip geometry adjacent to the rf washer SQUID, as sketched in Fig. 3. The substrate resonator is equipped with a YBCO thin film washer structure in order to adjust the resonance frequency to approximately 650 MHz and to enhance the magnetic field sensitivity.

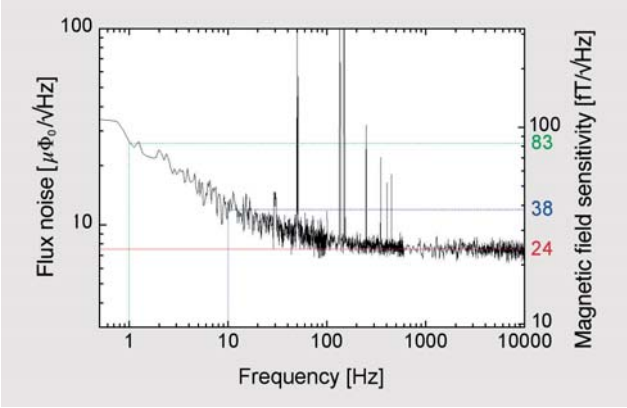

Fig. 4
Flux noise and magnetic field noise of a substrate resonator rf SQUID incorporating a YBCO step edge junction.

RESULTS

SQUID Sensor

Fig. 4 shows a noise measurement of the SQUID magnetometer with substrate resonator at 77K. The SQUID loop was 100 x 100 μm^2, this corresponds to a SQUID inductance of 150 pH. Because the flux concentrator (washer structure) uses the full resonator substrate area of 10 x 10 mm^2, we achieved a field-to-flux transfer coefficient $\partial B/\partial \phi$ of 3.2 nT/Φ_0. A white SQUID flux noise of 7.3 $\mu\Phi_0/\sqrt{Hz}$ was found, corresponding to a field sensitivity of 24 $fT/\sqrt{Hz}$. In the low frequency range, a noise figure of 38 $fT/\sqrt{Hz}$ at 10 Hz and 83 $fT/\sqrt{Hz}$ at 1 Hz is achieved (2). As the fabrication of the single layer SQUIDs is relatively simple, the substrate resonator concept offers a very practical and straightforward method to obtain high sensitivity SQUID magnetometers.

Eddy current non-destructive materials testing

Nonmagnetic metallic materials are usually tested by inducing eddy currents and measuring the magnetic field response. This inductive ac technique is based on a narrowband lock-in readout scheme, resulting in noise suppression and allowing to evaluate the quadrature component of the response field which contains information on excitation energy dissipation. In highly conductive materials, probing of deeper defects mandates using lower excitation frequencies. Sensitivity of induction coils decreases with frequency, so that SQUIDs can offer a higher sensitivity of detection of very deep faults (3).

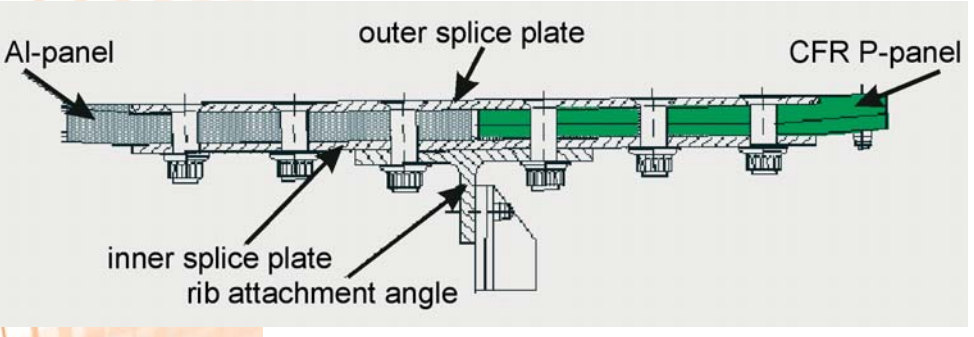

Fig. 5
Projected structure of the Airbus A380 wing splice, where the aluminium wing and the carbon fiber reinforced wing panel meet.

Fig. 6
Signal traces of the Airbus A380 wing splice sample, measured with SQUID (top) and induction coil (bottom) in conjunction with eddy current excitation.

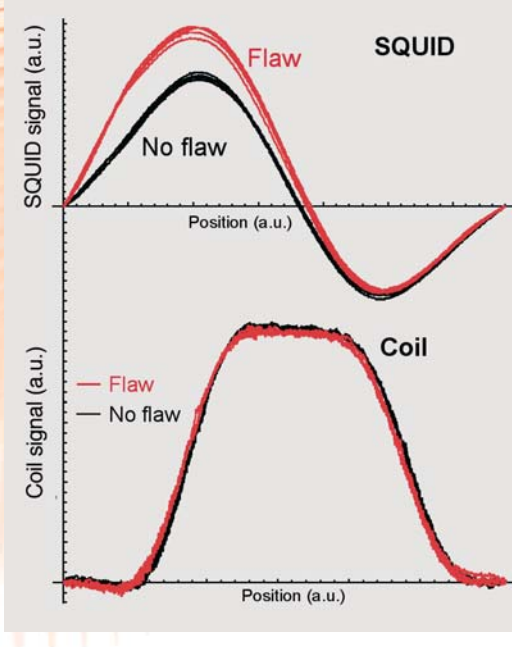

As the construction of the megaliner Airbus aircraft progresses, testing procedures for extremely thick-walled structures are needed. A bolted three-layer aluminium sample from EADS Airbus, modeling the projected outer wing splice of the Airbus A380 with a total thickness of 62 mm (Fig. 5), was measured with a Joule-Thomson machine-cooled SQUID. For sufficient current penetration into the layered aluminium sample, an excitation field in the range of 10 – 40 Hz was applied. The small field variations caused by the defects are superimposed on the current distortions and the corresponding field changes in the vicinity of the titanium bolts. Separation of these two contributions was achieved by signal processing. Fig. 6 (top) shows the measured SQUID line scan traces (after liftoff correction and phase optimization) in the case of a titanium bolt with an adjacent flaw (30 mm long, at a depth of 31 – 46 mm) and, for comparison, an unflawed bolt connection. The flawed bolt is easily identified. In contrast, it was impossible to distinguish between flawed and unflawed bolt in the corresponding measurement with a conventional commercial eddy current system (Fig. 6 bottom). Hence, the SQUID technique constitutes a powerful non-destructive method for the inspection of extremely thick aluminium structures.

Biomagnetic diagnostics: Magnetocardiography

Similar to electrocardiography (ECG), magnetocardiography (MCG) extracts clinically relevant information from the biosignals generated by the human heart. The cardiac cellular action potential initiates intra- and extracellular ion currents, giving rise to a magnetic field above the chest. The basic advantages of MCG over ECG is the high sensitivity to local myocardial currents, undisturbed by contact resistances at tissue boundaries. The diagnostic value has been shown in a number of medical studies, e.g. on MCG diagnosis of coronary artery disease, on myocardial infarction, on fetal MCG. As the magnetic signal of the human heart amounts to only about 100 pT (peak-to-peak) above the chest, a SQUID is required for MCG recordings. A 1997 study of the Research Center Jülich together with the Medical Clinic of the Technical University Aachen showed that MCG data allow to differentiate between a group of patients with coronary artery disease in conjunction with ventricular tachycardia and a healthy control group, thus allowing risc stratification of sudden cardiac death. This is significant because it is impossible to separate the groups on the basis of ECG data.

A major drawback of MCG, which probably has prevented MCG from finding widespread clinical use so far, is the necessity to conduct MCG measurements in a magnetically shielded room. Recently, we developed a first-order electronic gradiometer incorporating our novel dielectric substrate resonator rf SQUIDs with high field sensitivity (2). After adaptation of the gradiometer baseline to the specific environmental magnetic disturbances at the measurement location, it was experimentally verified that the system is well suited for performing MCG measurements in an unshielded environment. Fig. 7 shows our portable SQUID gradiometer system. The tripod holding the cryostat may be dismantled, the complete system fits into a travel suitcase. A typical

Fig. 7
Portable SQUID gradiometer system for recording human magnetocardiograms in unshielded enviromment.
The tripod holding the cryostat may be dismantled, the complete system fits into a travel suitcase.

Fig. 8
Typical MCG measurement recorded in unshielded environment. The real time signal is displayed with a video band-width of 30 Hz.

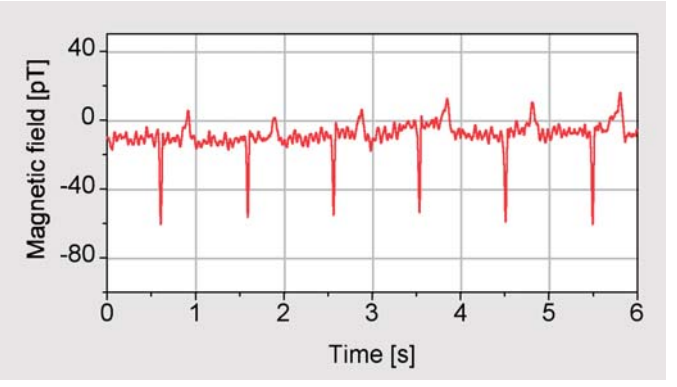

real-time MCG recording is displayed in Fig. 8. Our first-order portable HTS gradiometer utilizing substrate resonator rf SQUIDs may be upgraded to a commercial multichannel MCG system.

Biosensors: Magnetic nanoparticle detection

Immunological techniques, such as immunoassays, employ the highly specific interaction between antigenes and antibodies in conjunction with markers for the detection and quantification of specific biomolecules. Typically, fluorochromes, enzymes, or radioactive compounds are used as markers. Each method has intrinsic limits. High sensitivity fluorescence detection is very involved. Therefore the sensitivity of enzyme techniques is not always sufficient. The use of radioactive markers poses radiation hazards. Magnetic label-based bioassays have been identified as a very promising alternative. These markers comprise of an iron oxide core of a few tens or hundred nanometer diameter with a biocompatible surface coating. They are stable, non-toxic and they can be manipulated by a magnetic field, thus allowing to sort them rather easily. The particles are superparamagnetic. In case of monodispersed particles, their concentration in a test volume can be quantitatively determined by AC susceptometry. In order to determine the achievable sensitivity for a given magnetic field sensor, the minimum detectable magnetic moment was calculated as a function of the sensor – particle distance (Signal-to-noise ratio of 1 for frequency of 50 kHz and bandwidth of 1 kHz). In the case of small particle-to-sensor spacings of the order of a few mm, the sensitivity advantage of SQUIDs amounts to more than three orders of magnitude over an opti-

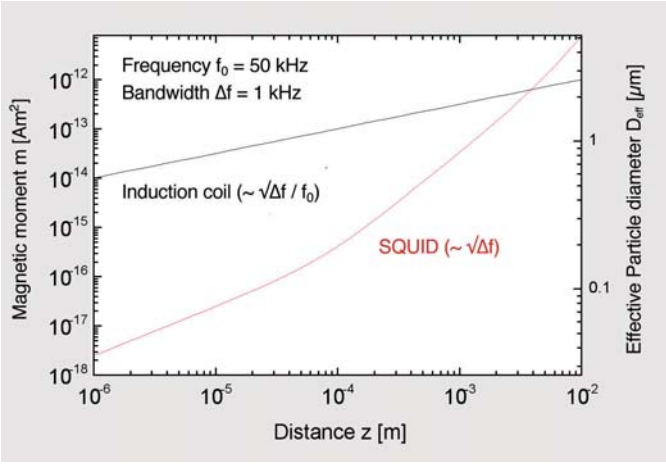

Fig. 9
Calculated mimimum detectable magnetic moment and corresponding effective particle by means of an optimized induction coil (black) or an optimized HTS SQUID sensor (red), as a function of the distance sensor – particle.

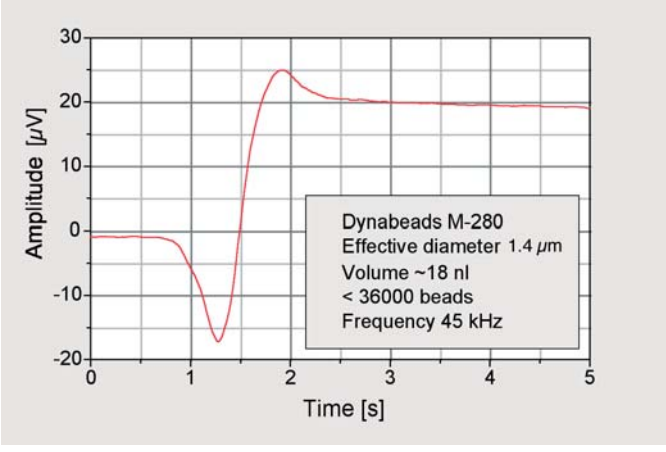

Fig. 10
AC susceptometry of 18 nl aqueous solution of Dynabead M-280 magnetic particles (effective iron oxide diameter 1.4 µm) with an induction coil. The solution was guided through a 150 µm diameter capillary close to the gap of a magnetic recording head, measuring the synchronous response to a 45 kHz excitation field.

mized induction coil (see Fig. 9). Fig. 10 shows the result of an induction coil measurement (using a magnetic recording head) of less than 36000 Dynabead M-280 magnetic particles (effective iron oxide diameter 1.4 µm) in aqueous solution in a 150 µm diameter capillary. Hence, with an optimized SQUID microscope, which is currently developed, the detection of single magnetic particles of about 100 nm diameter is possible. In addition, the setup allows to employ the so-called relaxometry technique. This method developed at the PTB Berlin allows to separate the contributions of bound and unbound magnetic particles in solution by measuring the time transient of magnetization relaxation. The Néel relaxation (reorientation of the magnetization vector inside the magnetic core) of the bound particles is governed by a significantly larger time constant than the Brownian relaxation of unbound particles.

REFERENCES

"SQUID Magnetometers"
A.I. Braginski, H.-J. Krause, J. Vrba,
in: "Handbook of thin film devices", Ed.: M.H. Francombe,
Volume 3, "Superconducting Film Devices",
Academic Press, San Diego (2000), pp. 149-225.

"Substrate resonator for HTS rf SQUID operation"
Y. Zhang, J. Schubert, N. Wolters, M. Banzet, W. Zander and H.-J. Krause
Physica C 372-376 (2002) 282-286.

"Recent developments in SQUID NDE"
H.-J. Krause and M. v. Kreutzbruck
Physica C 368 (2002) 70-79.

AUTHORS

Hans-Joachim Krause, Yi Zhang, Gregor I. Panaitov, Dieter Lomparski, Norbert Wolters, Jürgen Schubert, Willi Zander